

2002

R-410A Air Conditioning System With Microchannel Condenser

C. Y. Park

University of Illinois at Urbana-Champaign

P. S. Hrnjak

University of Illinois at Urbana-Champaign

Follow this and additional works at: <http://docs.lib.purdue.edu/iracc>

Park, C. Y. and Hrnjak, P. S., "R-410A Air Conditioning System With Microchannel Condenser" (2002). *International Refrigeration and Air Conditioning Conference*. Paper 556.
<http://docs.lib.purdue.edu/iracc/556>

This document has been made available through Purdue e-Pubs, a service of the Purdue University Libraries. Please contact epubs@purdue.edu for additional information.

Complete proceedings may be acquired in print and on CD-ROM directly from the Ray W. Herrick Laboratories at <https://engineering.purdue.edu/Herrick/Events/orderlit.html>

R-410A AIR CONDITIONING SYSTEM WITH MICROCHANNEL CONDENSER

C. Y. Park and, P. S. Hrnjak¹

ACRC - Air Conditioning and Refrigeration Center
Department of Mechanical and Industrial Engineering
University of Illinois at Urbana-Champaign

ABSTRACT

This paper presents experimental results from a prototype of a microchannel heat exchanger used in a residential air-conditioning system as an air-cooled condenser. The main objectives were to analyze effects of the microchannel condenser on system performance. The commercially available system that utilizes a condenser with a round tube and plate fins was experimentally evaluated first, then the original condenser was replaced with a microchannel heat exchanger of almost identical external volume, face area, and fin pitch. The performance of the systems and condensers were compared. Condenser performance was quantified in terms of the overall heat-transfer coefficient values for different experimental conditions. The cooling capacity of the system and the coefficient of performance were compared under the same conditions (air-flow rates, temperatures, and humidities). The cooling capacity as well as the coefficient of performance for the system with a microchannel condenser was improved under each of the conditions. The charge of system using microchannel condenser was 9% less than that of the system using round-tube condenser. The airside velocity and pressure difference distributions of both condensers are also shown.

1. INTRODUCTION

In professional circles, there is an ongoing debate about the potential benefits of using microchannel heat exchangers. There is an expectation that heat exchangers with small-channel flat tubes or with microchannel tubes would offer advantages over those with round tubes; but no experimental validation for R410A was found in the open literature. Some advantages were expected to come from substantial charge reductions, some due to a lower airside pressure drop, others from higher heat-transfer coefficients on the refrigerant side and even on the air side, as well as from greater airside surface area in a given volume. Fan power was also expected to be reduced because of the lower drag coefficients of the flat-tube design. The objective here is to address these issues.

Two heat exchangers were used as condensers in the same air-conditioning system, one with round tubes and the other with flat microchannel tubes in a parallel-flow arrangement. The differences were recorded and are explained herein. This paper presents the difference measured in the performance for both condensers only as well as the effects on the system. The microchannel heat exchanger was made to have nearly a identical face area, depth and consequently volume, plus the same fin density as the baseline, round-tube heat exchanger with plate fins. The baseline condenser along with all other elements of the system were part of the very generously sized, off-the-shelf, air-conditioning system manufactured by one of the market and technology leaders. The system had a scroll compressor, like those typically used in applications such as this (ZP32K3E-PFV-230) and orifice tube used as an expansion device. The baseline system has been examined in detail earlier and presented in a few publications which compared it to a prototype of the transcritical CO₂ system (Beaver et al. 1999, 2000). In the present study, the performance of the baseline system and prototype system was measured under the conditions specified above. All measurements were taken for both systems within a short period of time in the same facility and under identical conditions. Many points were repeated in order to assure the correctness of the results.

The measured data for the baseline system showed a slightly reduced efficiency for the same scroll compressor used earlier, which is believed to be caused by the specific history of the compressor used to run experiments in the transcritical mode with R410A (Yin, Bullard and Hrnjak, 2000).

¹ Author to whom correspondence should be sent: pega@uiuc.edu.

2. HEAT EXCHANGERS EXAMINED

Fig. 1 presents a photograph of the two heat exchangers used as condensers, one with round tubes and plate fins; the other, with microchannel tubes in parallel flow. They have almost identical shapes, volumes, face areas, and fin densities.

Detailed characteristics are given in Table 1. A schematic showing the circuiting is shown in Fig. 2. A microchannel condenser has three paths, as shown. The number of tubes for each path is smaller as the refrigerant flows, thus decreasing the flow area. A round-tube condenser has two paths. The first path consists of two circuits; one with an upward flow, and the other with a downward flow. By merging the two circuits at the inlet of second path, the flow area is reduced by half. The fins applied in a round-tube condenser are offset-strip fins; the fins in a microchannel condenser are folded and louvered.

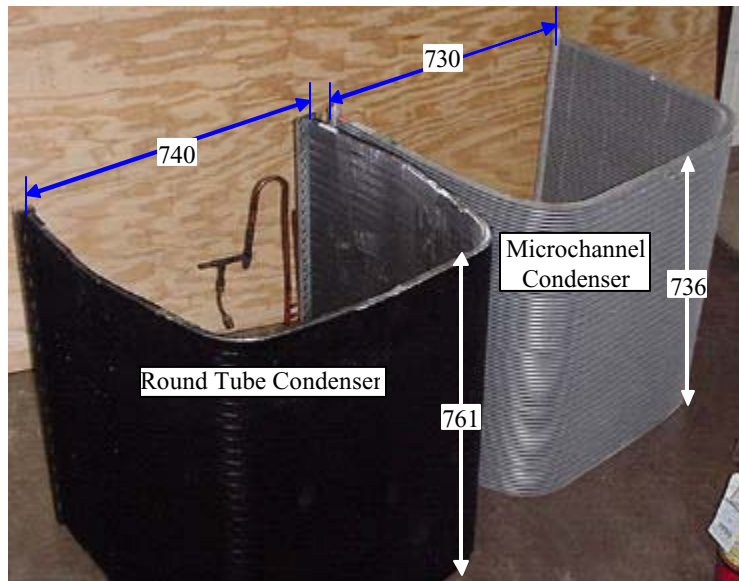


Fig. 1. The two condensers used

Fig. 3 shows the fins in a round-tube condenser and microchannel condenser. The fin spacing is very narrow: 1mm (24 fpi). The air side enhancements are typical used in these application: offset-strip fins for the round-tube plate fin heat exchanger and louver folded fin for parallel flow microchannel heat exchangers.

The rest of the system was unchanged in experiments focused to condenser.

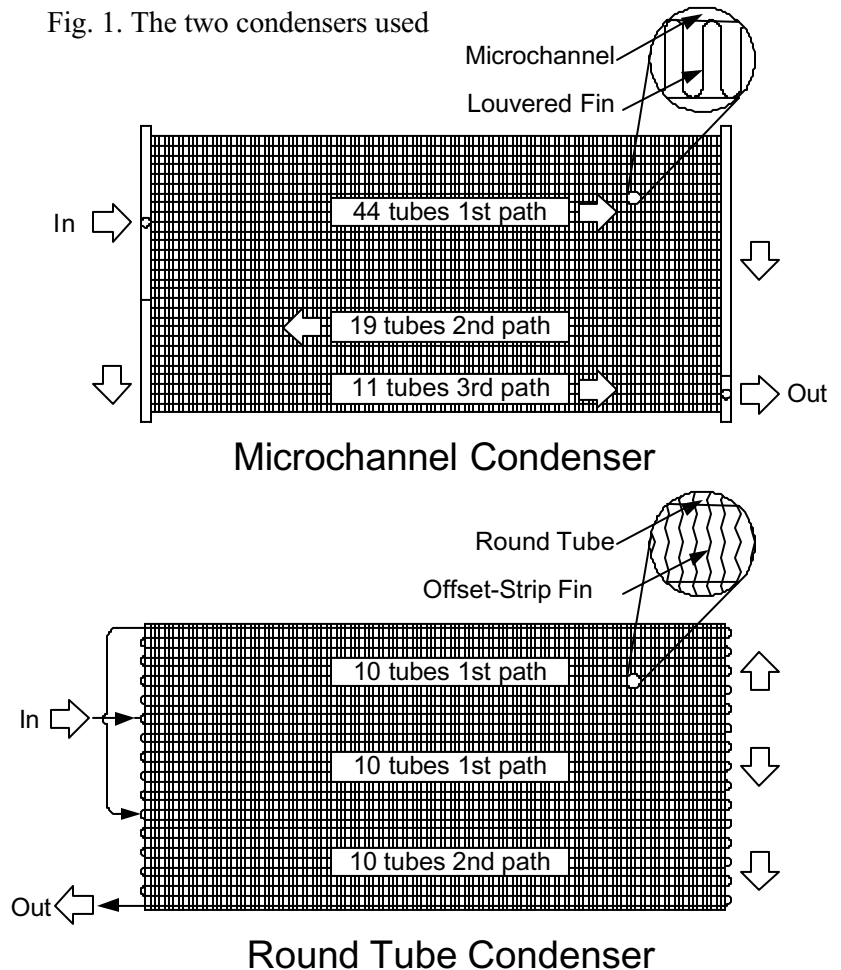


Fig. 2. Schematics of the unfolded condensers.

Table 1. Geometric characteristics for the two condensers and the evaporator.

	Round tube condenser	Microchannel condenser	Evaporator
Face area [m ²]	1.43	1.32	0.32
Core depth [m]	0.0191	0.021	0.056
Core volume [m ³]	0.0273	0.0277	0.018
Airside area [m ²]	45.04	46.06	18.6
Ref. side area [m ²]	1.5	9.11	1.0
Fin spacing	1 mm (24 fpi)	1 mm (24 fpi)	1.7 mm
Fins	offset-strip plates	louvered folded	wavy plate
Fin material	Al	Al	Al
Tube material	Cu	Al	Cu
Tube OD [mm]	9.5	1.9(height) 21(width)	9.5
Tube number	30	74	84
Tube rows	1	1	3
Paths	1st : 2 circuits 10 tubes each 2nd : 1circuit 10 tubes	1st : 44 tubes 2nd : 19 tubes 3rd : 11 tubes	6 independent circuits 14 tubes each

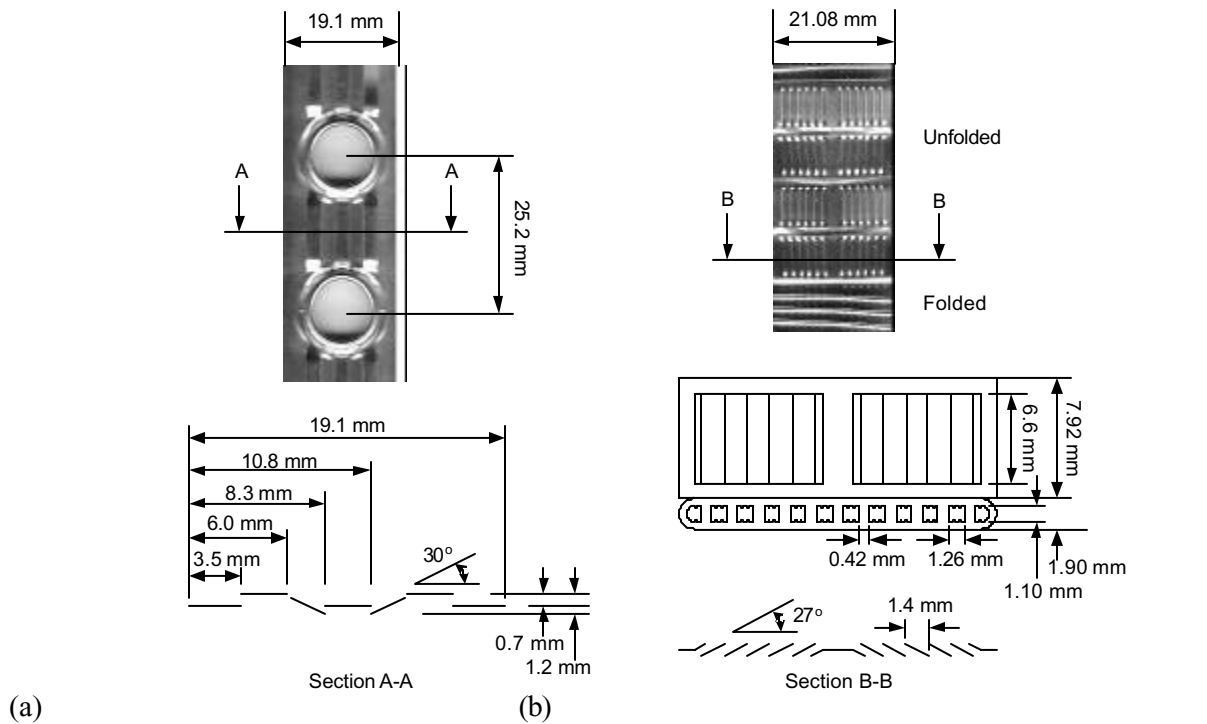


Fig. 3. (a) Offset-strip fins for the round-tube condenser, (b) Louver folded fin and microchannel dimension used in the microchannel condenser.

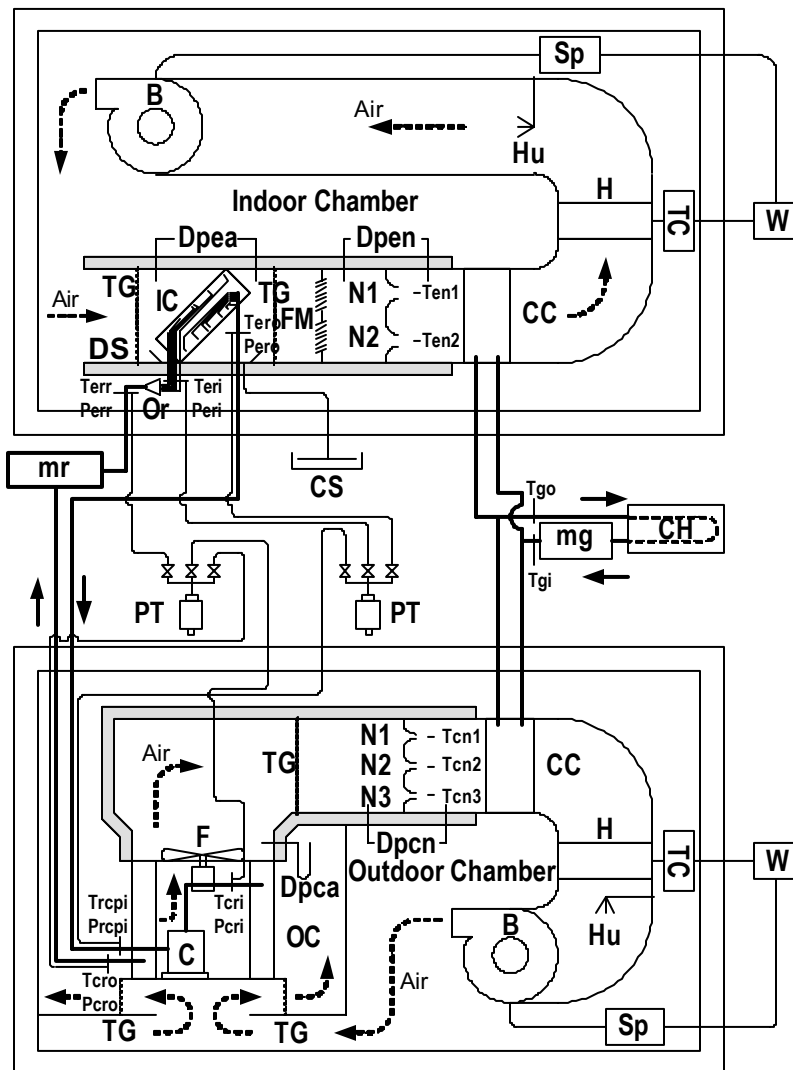
3. SYSTEMS EXAMINED

All elements of the baseline system were part of the very generously sized, off-the-shelf, air-conditioning system manufactured by one of the market and technology leaders. The system used a hermetic scroll compressor (ZP32K3E-PFV-230) and an orifice tube (ID=1.78 mm) as an expansion device. The system used was critically charged and had no receiver. The standard condition for charging the system is the superheat of the evaporator exit, 2.8°C at ARI Condition A. In addition to that nominal value, the charge was varied in order to obtain a better understanding of the effect caused by subcooling (charge) on performance.

4. EXPERIMENTAL FACILITY

Separate environmental chambers were constructed for each heat exchanger. Three independent methods for determining capacity were utilized in both the indoor and outdoor chambers: chamber calorimetry, airside energy balance, and refrigerant side energy balance. The test facilities are described in detail by Beaver et al. (1999). A schematic of the test facility is given in Fig. 4.

The controllers in the two environmental chambers maintained outdoor and indoor temperatures within $\pm 0.3^\circ\text{C}$ and absolute humidity at $\pm 2\%$. A variable-speed wind tunnel in each chamber simulated the range of operating conditions encountered in real applications, and allowed a measurement of the air-flow rates within $\pm 1\%$. A Coriolis-type, mass-flow meter together with immersion thermocouples and electronic pressure transducers measured the pressures upstream and downstream of every component, yielding refrigerant-side capacity determinations repeatable within $\pm 2\%$.



- B – Blower
- C – Compressor
- CC – Cooling Coil
- CH – Glycol Chiller
- CS – Condensate Scale
- Dp – Differential Pressure Transducer
- DS – Dew Point Censer
- F – Fan
- FM – Flow Mixer
- H – Heater
- Hu – Humidifier
- IC – Residential Indoor Coil
- mg – Glycol Mass Flow Meter
- mr – Refrigerant Mass Flow Meter
- N – Nozzle
- OC – Outdoor Condenser
- Or – Orifice
- PT – Pressure Transducer
- Sp – Speed Controller And Tachometer
- T – Temperature
- TC – Temperature Controller
- TG – Temperature Grid
- W – Watt
- a – Air
- c – Condenser
- cp – Compressor
- e – Evaporator
- g – Glycol
- i – Inlet
- o – Outlet
- r – Refrigerant

Fig. 4. Experimental setup.

Room calorimetry was the most accurate: the walls were made of 30cm thick polyurethane with five thermocouples on both sides of the wall, floor, and ceiling of each environmental chamber. Heat losses were carefully calibrated so that error was held within $\pm 0.1\%$ of the total system capacity (approximately 10 kW). All dry-energy inputs (electric) were measured by watt transducers with a $\pm 0.2\%$ full-scale accuracy. The test results showed agreement between the independently determined capacities to be within $\pm 3\%$, with the error due primarily to uncertainties in the airside calorimetry.

5. TEST-MATRIX AND SYSTEM RESULTS

Three main test conditions were used for system comparison: A, B, and C as defined in the ARI 210/240 standard. All test conditions require an indoor temperature of 26.7°C for the a/c mode. The indoor humidity for the standard capacity-rating condition (A) and the steady-state condition (B) is 50% ($T_{wb} = 19.4^\circ\text{C}$). For steady-state, dry-coil tests, (C) indoor humidities must be less than 22% ($T_{wb} < 13.9^\circ\text{C}$). The ARI standard 210/240 also recommends a maximum operation condition test at $T_{outdoor} = 46.1^\circ\text{C}$, $T_{wb} = 23.9^\circ\text{C}$. The ASHRAE Standard 116/1995 prescribes a test point at $T_{indoor} = 26.7^\circ\text{C}$, $T_{outdoor} = 35^\circ\text{C}$ for condition A, and $T_{outdoor} = 27.8^\circ\text{C}$ for conditions B and C as the rating point for the system. This setup was further expanded in order to provide data for the component analysis as well as to verify the model predictions.

Fig. 5 compares the capacity Q and coefficient of performance, COP, for the R410A baseline system (with a round-tube condenser) and for the improved system (with a microchannel condenser) at three rating conditions (A, B, and C). Under condition A, the evaporator capacity and COP of the microchannel condenser were 4.3% and 18.8% higher, respectively than those of the round-tube heat exchanger under condition A. The results of Fig. 5 were based on the system subcooling, 8.9°C and 6.9°C , for each round tube and microchannel condenser system under condition A. The air-flow rates over the condenser and the evaporator were constant, done by adjusting the auxiliary blower speed. That option for initial comparison was chosen so as to provide airside balance as the third independent method for determining condenser capacity.

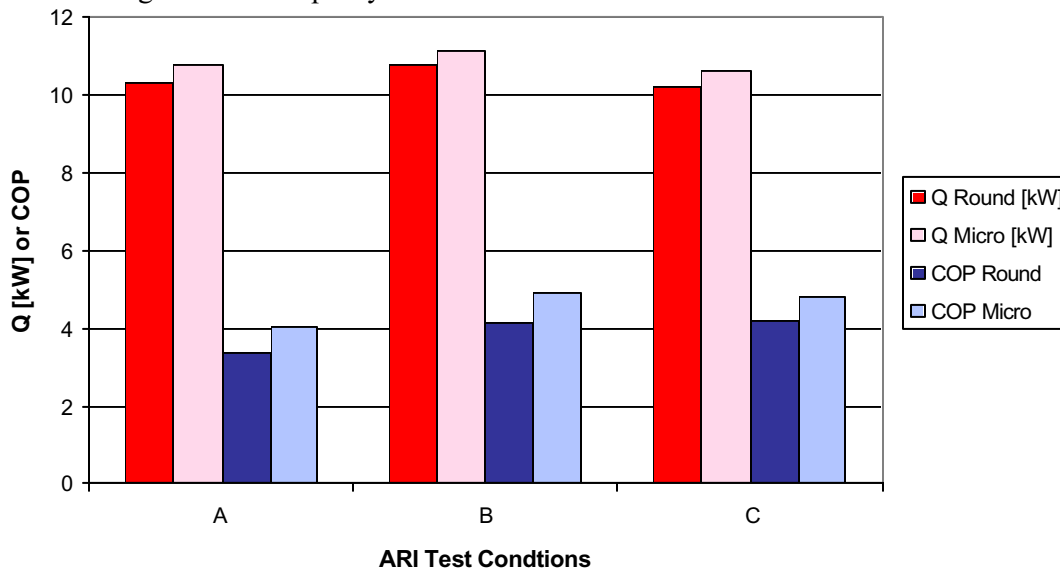


Fig. 5. Comparison of system data - capacity Q and coefficient performance (COP) - for the same system with the round-tube condenser and the microchannel parallel-flow condenser under ARI condition A, B, and C. The air-flow rate was the same.

The experimental results showed that the system was somewhat sensitive to subcooling, as expected in a system without a receiver. Subcooling was a consequence of the charge. Some experiments were

performed with the different subcooling and almost the same superheat of the evaporator under test condition A. Fig. 6 shows the relation of subcooling and COP. At any subcooling, the COP of the system using a microchannel condenser was 10.0% ~ 20.6% higher than the COP when using a round-tube condenser.

Fig. 7 show the cycle comparisons for both systems with T-h and p-h diagrams for ARI conditions A. All values were derived experimentally. We selected the slightly unusual T-h format because it illustrates better the operation of heat exchangers. The dotted lines represent changes in air temperatures over the condenser and evaporator. These graphs clearly indicate the effects of using a microchannel condenser on the performance of the system. As is obvious, the condensing temperature (pressure) was reduced because of a better heat transfer plus lower refrigerant-side pressure drop. Both results increased compressor and cycle efficiency and consequently, the COP.

With condition A, the condensing temperature of the microchannel condenser was 2.3°C less than that of the round-tube condenser. The higher condensing temperature reduced compressor efficiency and COP. For the conditions presented in Fig. 7, the microchannel condenser produced improvements of 3% in cooling capacity, 1.6% in condenser capacity, and 15% in COP, compared to values for the round-tube condenser.

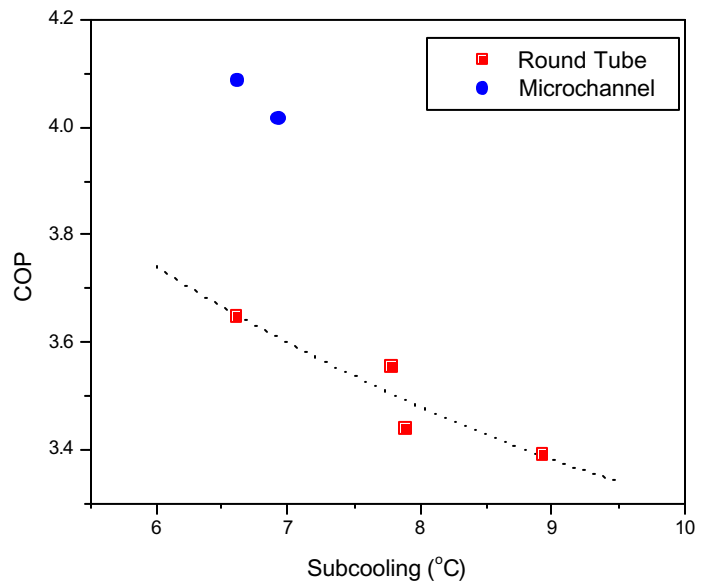


Fig. 6. The relation of COP and subcooling

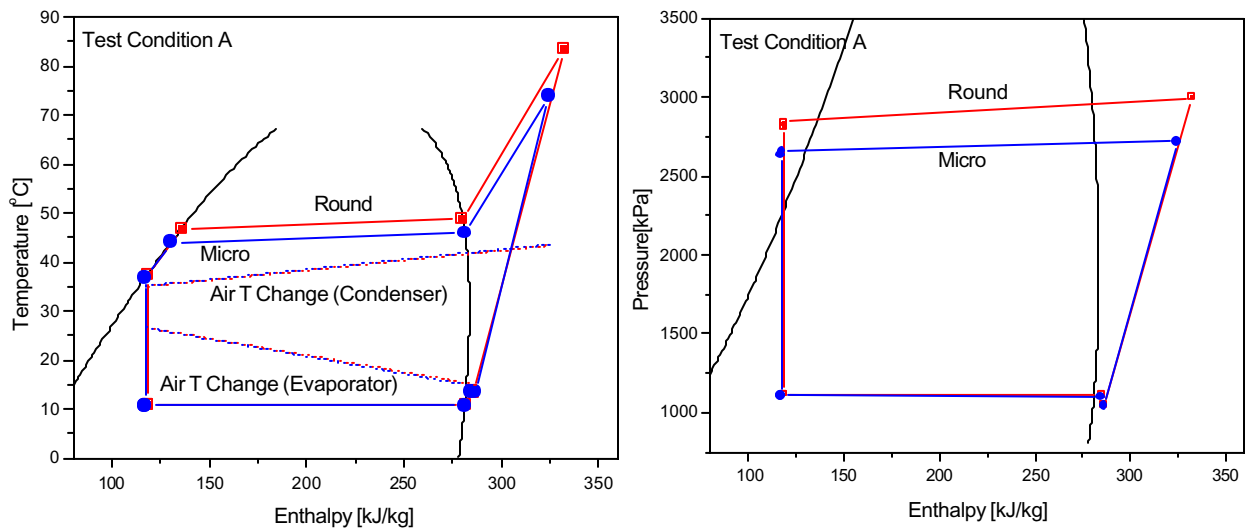


Fig. 7. Cycle comparison: ARI condition A, effect of two condensers on systems

Also, the refrigerant pressure drop of the microchannel condenser was 68% less than that of the round-tube condenser. Clearly, this explains the frequently noted misconception that condensers with small-diameter tubes have a higher refrigerant-side pressure drop than those with larger tubes. The effect of reducing the diameter is offset by the increased number of parallel channels. Certainly, the limit in controlling the refrigerant-side pressure drop in a parallel-flow microchannel condenser is a single-pass arrangement.

6. HEAT-TRANSFER PERFORMANCE

Overall heat-transfer performance measurements were taken for each condenser and for the system. Overall condenser performance was quantified in terms of U_{air} values for different subcooling and test conditions. The overall heat-transfer coefficients based on the airside area, U_{air} , are shown in Figs. 17 and 18. The value for U_{air} was calculated by dividing the total heat transfer by the log mean temperature difference, LMTD, which neglects superheating and subcooling in the condenser. Even being aware of simplifications of this approach, we are providing this variable for a designer who can make an easy calculation for total heat transfer by multiplying the coefficient times the airside area and the LMTD of the application, and then compare it to conventional condensers. Further justification of the simplification is the purpose of comparing two heat exchangers based on data under the same conditions. Detailed modeling results will be presented in a separate publication.

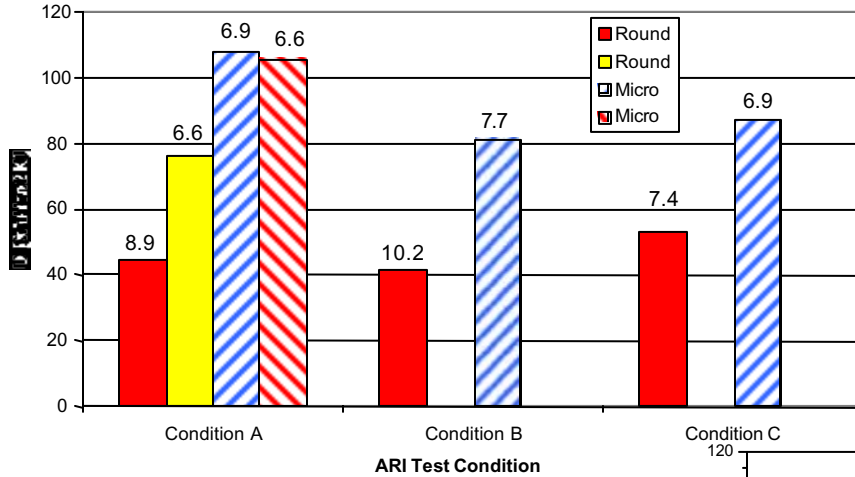


Fig. 17. ARI conditions A, B, and C: overall heat-transfer coefficients in the microchannel and the round-tube condensers. The values on the bar represent subcooling under each condition.

The value for U_{air} is affected somewhat by the amount of refrigerant subcooling. Refrigerant single-phase heat transfer is more than an order of magnitude smaller than in two-phase transfer. The larger the region occupied by liquid, single-phase refrigerant, the higher the refrigerant-side heat transfer resistance due to a reduced two-phase area. This results in lower values for U_{air} . Figs. 17 and 18 show this trend. With condition A, the U_{air} of the round-tube condenser is 72.9% higher in the case when the subcooling is 6.6 °C than in subcooling 8.9 °C. When the subcooling is 6.6 °C under test condition A, the U_{air} of the microchannel condenser is 38.0 % higher than that of the round-tube condenser.

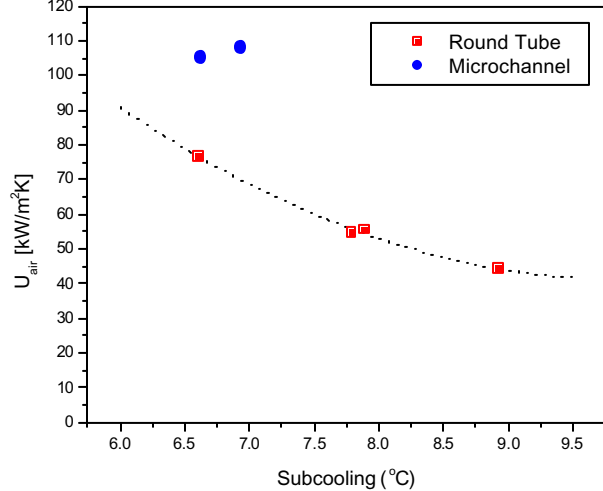


Fig. 18. Overall heat-transfer coefficients in the microchannel and the round-tube condensers under certain subcooling conditions

7. REFRIGERANT INVENTORY

Table 2 presents measured and derived data for refrigerant inventory. Greater reduction of inventory when using microchannel condenser was expected. It appears that significant fraction of refrigerant is in the headers.

8. SUMMARY AND CONCLUSIONS

The objective of this work was to experimentally compare and explain differences between a microchannel condenser and a round-tube condenser, their effects on system performance in a real-world application, and shed the light on the potential benefits of using microchannel heat exchangers. A

prototype of a microchannel condenser was constructed, experimental heat-transfer and pressure-drop measurements were taken for two types of condensers: a round-tube unit and a parallel-flow microchannel tube unit. Comparisons between the two very similarly sized, almost identical condensers showed the superiority of the microchannel design. Even though the project was done with only one prototype under various conditions, the conclusions could be generalized based on the analysis presented.

Table 2. The comparison of system and condenser charge amount

System with condenser type	Evaporator capacity [kW]	Total charge [g]	Specific charge based on evaporator capacity [g/kW]	Condenser capacity [kW]	Condenser charge [g]	Specific charge for condenser [g/kW]
microchannel	10.49	2655.5	253.15	13.26	1233	93.06
round tube	10.46	2925	279.64	13.14	1512.5	115.11

Our experimental results indicated that the microchannel condenser improves COP, condenser capacity, and evaporator capacity, compared to the baseline system using a round-tube condenser. These contributions are caused by the superior heat-transfer characteristic of a microchannel condenser, lower refrigerant-side pressure drop, and consequently lower condensing temperature - resulting in requiring less work from compressor. That gives the higher system capacity and COP.

The air-velocity distribution on the surface of the two condensers was similar, and that distribution is related to the distance between the condenser fan and the condenser surface. The dead zones of air-flow were measured in corners of the condensers and in the folded parts. The airside pressure drop distribution matched well with the distribution of velocity. In this study, the value of U_{air} decreased as subcooling increased; and this phenomenon is physically valid.

9. ACKNOWLEDGMENTS

The authors greatly acknowledge funding by the Modine Manufacturing Co., and support by form the Carrier and Copeland companies for this project. The assistance of Dr. Jianmin Yin was of great importance for timely and accurate results, and authors express their great appreciation.

10. CONTACT

Pega Hrnjak, Res. Professor, Co-Director ACRC, University of Illinois at Urbana-Champaign, 1206 W. Green St. Urbana, IL 61801, USA, e-mail: pega@uiuc.edu.

11. REFERENCES

- ANSI/ASHRAE Standard 116, 1995. Method of testing for seasonal efficiency of unitary air-conditioners and heat pumps, American Society of Heating, Refrigeration and Air -Conditioning Engineers, Inc.
- ARI Standard 210/240, 1989. Standard for unitary air conditioning and air source heat pump equipment, Air Conditioning and Refrigeration Institute
- Beaver, A.C., Yin, J.M., Bullard, C.W., and Hrnjak, P.S., 1999 "An Experimental Investigation of Transcritical Carbon Dioxide Systems for Residential Air Conditioning," University of Illinois at Urbana-Champaign, CR-18.
- Beaver, A.C., Yin, J. M., Bullard, C. W., and Hrnjak, P. S., 1999 "Experimental and Model Study of the Heat Pump/Air Conditioning Systems Based on Transcritical Cycle with R744," *Proceedings of 20th International Congress of Refrigeration*, Sydney Australia.
- Yin, J. M., Bullard, C. W., and Hrnjak, P. S., 2000. Performance of transcritical and subcritical R410A residential a/c and h/p system. *Proceedings of the Purdue Refrigeration Conference*, pp. 169-176.